

Article

Structural Elucidation of Azo and Quinoneimine Products Formed in Diazonium-Based Color Reactions of Cannabinoids

Hikari Nishiguchi ¹, Kayo Nakamura ^{1,*} , Ryosuke Arai ¹, Riho Hamajima ¹, Hiroko Abe ², Akihiko Ishida ³ , Manabu Tokeshi ³ , Kyohei Higashi ¹ , Akiyoshi Saitoh ¹ and Hideyo Takahashi ^{1,*} 

¹ Faculty of Pharmaceutical Sciences, Tokyo University of Science, 6-3-1 Niijuku, Katsushika-ku, Tokyo 125-8585, Japan

² BioDesign Inc., IB Daiichi-Bld 6th Floor, 3-25-15 Nishi-Ikebukuro, Toshima-ku, Tokyo 171-0021, Japan

³ Faculty of Engineering, Hokkaido University, Kita 13, Nishi 8, Kita-ku, Sapporo 060-8628, Japan

* Correspondence: kayo_nakamura@rs.tus.ac.jp (K.N.); hide-tak@rs.tus.ac.jp (H.T.); Tel.: +81-3-5876-1787 (H.T.)

Abstract

Cannabis use is generally restricted worldwide because it contains the narcotic compound Δ^9 -tetrahydrocannabinol (Δ^9 -THC). Although cannabis is detected at crime scenes using color-based primary screening methods, the details of the reaction mechanism have not yet been elucidated. In this study, we isolated the products generated during the color reaction between the diazonium salt prepared from *para*-nitroaniline and nine cannabinoids and determined their structures. Azo compounds **6**, **11**, **16**, and **17** were produced from cannabidiol, cannabigerol, cannabichromene, and cannabidiolic acid, respectively, while quinoneimines **7–10** and **12–15**, which contained positional isomers, were produced from cannabinol, Δ^9 -THC, and hexahydrocannabinol. The reaction barely proceeded with Δ^9 -THC acetate and HHC acetate.

Keywords: cannabis; color reaction; diazo coupling; cannabinoid; cannabidiol; cannabinol; Δ^9 -tetrahydrocannabinol; hexahydrocannabinol; cannabigerol; cannabichromene

1. Introduction

Cannabis has long been used in a wide range of fields, including medicine and pharmacology [1]. The compounds present in cannabis are called cannabinoids, and more than 100 types have been reported [2]. Figure 1a shows the structures of major cannabinoids. However, because the narcotic effects of Δ^9 -tetrahydrocannabinol (Δ^9 -THC) in cannabis have become clear, Δ^9 -THC is regulated worldwide, and its possession and use are prohibited in Japan. Despite this, the number of arrests for cannabis-related crimes remains high according to a recent report from the Japanese Ministry of Health, Labor, and Welfare [3]. Consequently, the number of illegal drug appraisals remains high, placing a strain on appraisers. Therefore, screening seized materials prior to accurate analysis is useful for improving appraisal and accelerating the arrest of cannabis-related offenders. Currently, cannabis is detected using color reactions as the primary screening method [4]. Various such reactions exist, the most well-known of which are the Beam [5], Ghamrawy [6], Duquenois [7], and diazo-coupling reactions [8], but there are many false positives. One of the reasons for this is the insufficient knowledge of the reaction products and mechanisms; that is, only estimated structures are available, and reports investigating the exact products and yields are scarce. Among these color reactions, we focused on the diazo-coupling reaction. Figure 1b shows the examples of coloring reagents.



Academic Editor: Alexander F. Khlebnikov

Received: 9 January 2026

Revised: 1 February 2026

Accepted: 24 February 2026

Published: 27 February 2026

Copyright: © 2026 by the authors.

Licensee MDPI, Basel, Switzerland.

This article is an open access article distributed under the terms and conditions of the [Creative Commons Attribution \(CC BY\) license](https://creativecommons.org/licenses/by/4.0/).

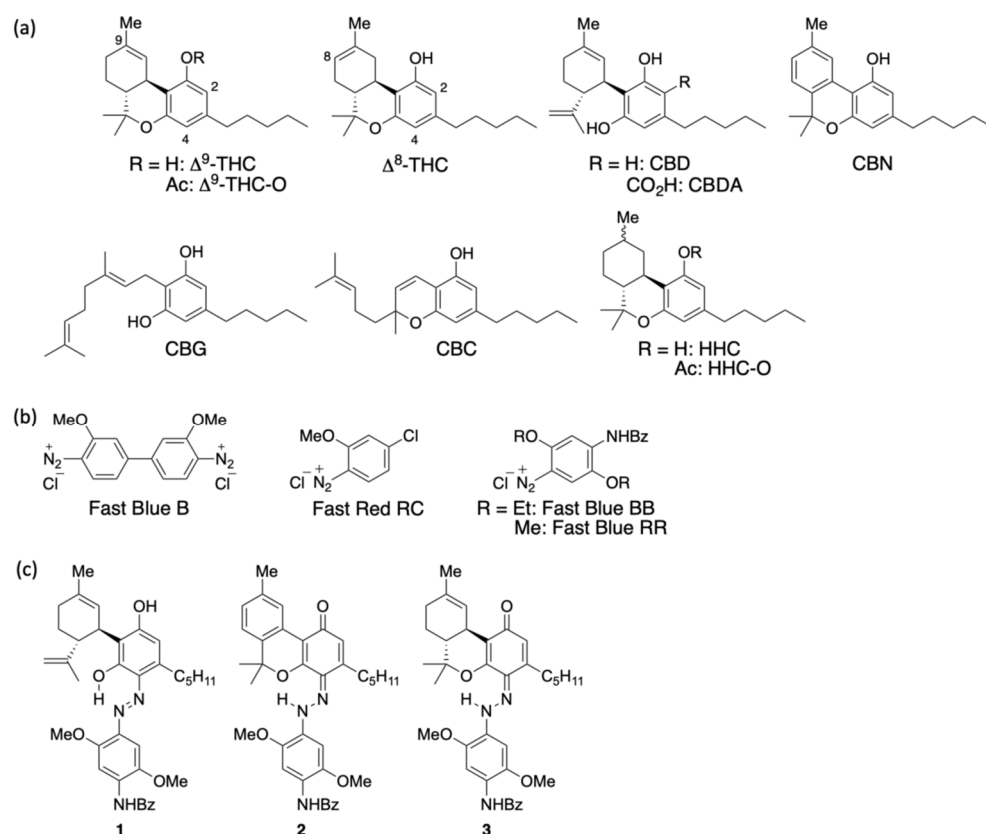


Figure 1. Structures of (a) cannabinoids, (b) coloring reagents, and (c) colored products.

In 1974, Sehon et al. reacted Δ^9 -THC with a diazonium salt prepared from *para*-aminobenzoic acid, and isolated a compound with an azo group attached at the 2-position [9]. However, the analytical technology available at the time was limited to mass spectrometry, elemental analysis, infrared spectroscopy, and ^1H NMR measurements; consequently, no ^{13}C NMR, 2D NMR, or X-ray diffraction structural data were available. Furthermore, the authors reasoned that the reaction occurred at the 2-position owing to the high reactivity of the *ortho*-position of phenol with insufficient evidence to fully determine the structure. In the same year, Fike et al. reported the isolation of a compound from the reaction of Δ^8 -THC with Fast Blue B [10]. They determined that the azo group was bonded at the 2-position of Δ^8 -THC based on the disappearance of the signal of the 2-position of Δ^8 -THC in the ^1H NMR spectrum. Considering that typical diazo-coupling reactions proceed at the *para*-position of the phenol, these regioselectivities are questionable. In 2019, Luo et al. performed LC-MS/MS analysis of the reaction solution of Δ^9 -THC and Fast Red RC, which revealed the production of two positional isomers bonded at 2- and 4-positions [11]. More recently, in 2020, Almiral et al. isolated the reaction product of Δ^9 -THC and Fast Blue BB, and reported that the signal at the 4-position of Δ^9 -THC disappeared in the ^1H NMR spectrum, indicating that the compound had a diazonium salt bonded at the 4-position [12]. This differs from the regioselectivity reported by Fike et al., who rationalized the structure based on the same analytical method. Furthermore, the ^1H NMR and COSY spectra of both studies were measured in deuterated methanol, which obscured signals from hydroxyl groups, and there were no ^{13}C NMR and other 2D NMR data available. Therefore, it is clear from the above discussion that further investigation is needed to determine the structure(s) of the diazo-coupling reaction products of cannabinoids.

In our previous study, we determined the structure of the products from the diazonium salt Fast Blue RR with the three major cannabinoids: cannabidiol (CBD), cannabinol (CBN), and Δ^9 -THC [13]. Specifically, the reaction with CBD produced azo compound **1** with the predicted structure, while CBN and Δ^9 -THC produced quinoneimines **2** and **3**, which are isomers of the azo compound (Figure 1c). In this study, we further investigated the trends of the diazo-coupling reaction and isolated and determined the structures of the reaction products of nine cannabinoids: CBD, CBN, Δ^9 -THC, cannabigerol (CBG), cannabichromene (CBC), hexahydrocannabinol (HHC), Δ^9 -THC acetate (Δ^9 -THC-O), HHC acetate (HHC-O), and cannabidiolic acid (CBDA). HHC, Δ^9 -THC-O, and HHC-O are semisynthetic cannabinoids and were chemically synthesized. HHC is found in very small amounts in cannabis plants, whereas Δ^9 -THC-O and HHC-O are not [14]. However, they are available on the market, so they are cannabinoids that need to be detected.

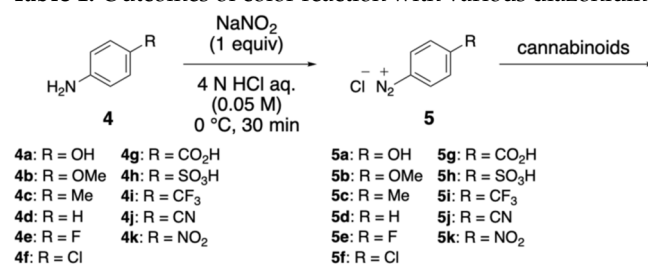
2. Results and Discussion

2.1. Color Reaction with Diazonium Salt

To investigate the color reaction with diazonium salts, reactions of simple diazonium salts bearing various *para*-substituents were attempted. Diazonium salt **5** was prepared by adding sodium nitrite to a hydrochloric acid solution of commercially available aniline **4**. Ethanol solutions of each cannabinoid were then added, and the color was observed (Table 1). In all entries, CBD and CBG, Δ^9 -THC and HHC, and Δ^9 -THC-O and HHC-O exhibited nearly identical colors. In particular, Δ^9 -THC-O and HHC-O, in which the phenols were protected by an acetyl group, showed no change in color from the blank in Entries 1–5 and a minimal change in Entries 6–11, indicating nearly no reaction. This indicates that free phenol is important for the reaction with diazonium salts. This is because acetyl group protection reduces the electron-donating ability of the cannabinoid benzene ring, thereby reducing its reactivity. Furthermore, in Entries 3 and 9–11, CBD, CBN, and Δ^9 -THC are distinguishable by color. This suggests that diazonium salts bearing alkyl- or electron-withdrawing groups have improved discrimination ability. Although it is difficult to interpret the effect of an alkyl group, in the case of electron-withdrawing groups, the decrease in the electron density of the diazonium salt may be responsible for the increase in reactivity. In our previous report, we revealed that the isolated compounds can be distinguished by color [13]. Therefore, it was expected that diazonium salts with electron-withdrawing groups would be more reactive with higher yields of reaction products that enable color identification. Presumably, the halogen groups in Entries 5 and 6 were not sufficiently electron-withdrawing, and the acidic protons in Entries 7 and 8 prevented color differentiation. It should be noted that because this method uses freshly prepared diazonium salts, it is not suitable for use at actual crime scenes. This study was conducted to clarify the characteristics of the color reaction used in conventional detection methods.

2.2. Isolation and Structural Determination of the Reaction Products

In the previous section, it was suggested that cannabinoids can be distinguished by color using diazonium salts with electron-withdrawing groups. This is speculated because the structure and yield of the reaction product would differ depending on the type of cannabinoids. To verify this, we isolated and determined the structure of the products of the reactions between different cannabinoids and the diazonium salt **5k** prepared from *para*-nitroaniline, which resulted in the most distinguishable color changes.

Table 1. Outcomes of color reaction with various diazonium salts.

| Entry | R | Result ¹ | Entry | R | Result ¹ |
|-------|-----|---------------------|-------|-------------------|---------------------|
| 1 | OH | | 7 | CO ₂ H | |
| 2 | OMe | | 8 | SO ₃ H | |
| 3 | Me | | 9 | CF ₃ | |
| 4 | H | | 10 | CN | |
| 5 | F | | 11 | NO ₂ | |
| 6 | Cl | | | | |

¹ a: blank, b: CBD, c: CBG, d: CBN, e: Δ⁹-THC, f: HHC, g: CBC, h: Δ⁹-THC-O, i: HHC-O, and j: CBDA.

2.2.1. Colored Product **6** from the Reaction of CBD with the Diazonium Salt **5k**

para-Nitroaniline was first treated with sodium nitrite and hydrochloric acid in an aqueous solution, followed by stirring for 30 min to generate the corresponding diazonium salt. The resulting diazonium salt was reacted with CBD in an ethanolic NaOH solution. Upon purification, a purple mixture was obtained. Thin-layer chromatography (TLC) indicated the almost complete consumption of CBD within 15 min, accompanied by the appearance of a new spot. Compound **6** corresponded to a yellow spot with an R_f value of 0.38 (hexane/ethyl acetate = 5/1) and was subsequently isolated by silica gel column chromatography. Figure 2 presents the key HMBC correlations for the isolated compound **6**. The ¹H NMR spectrum of **6** showed 33 proton signals, and the integration values indicated that **6** was formed from CBD and one equivalent of *para*-nitroaniline. A strong downfield resonance at 15.76 ppm was observed and was attributed to a hydrogen bond to either the oxygen or nitrogen atom. This pattern was similar to that of compound **1**, and **6** was likely to be an azo compound. HMBC correlations were observed between this proton signal and the carbon peaks at 164.6, 132.0, and 115.6 ppm. As these peaks were assigned to the benzene carbon atoms of CBD, the proton signal at 15.75 ppm corresponds to the proton of phenol bonded to the benzene ring derived from CBD. This phenol peak shifted downfield due to the formation of a hydrogen bond with the lone pair of the azo group. Therefore, **6** was determined to be an azo compound with two phenol groups and was isolated in quantitative yield. Product **6** is consistent with our previous report on the reaction of CBD with Fast Blue RR; however, whereas Fast Blue RR produced a moderate yield and a small amount of the disubstituted product, the reaction with the diazonium salt

prepared from *para*-nitroaniline afforded only the monosubstituted product quantitatively. When an excess of the diazonium salt of *para*-nitroaniline was reacted with compound **6**, no disubstituted compound was formed. It is presumed that the attachment of the azo group to the strongly electron-withdrawing nitro group reduced the electron density of the benzene ring of CBD, preventing the second reaction from proceeding. The formation mechanism of **6** is presumed to entail the addition of a diazonium salt, followed by rearomatization (Scheme 1).

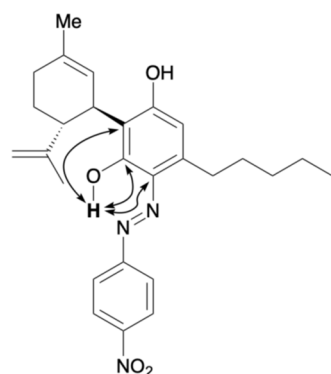
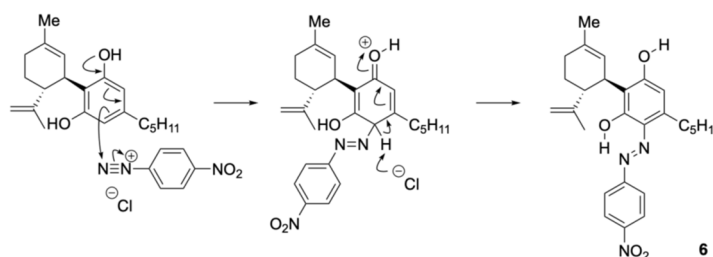


Figure 2. Key HMBC correlations for **6**.



Scheme 1. Proposed formation mechanism of **6**.

2.2.2. Colored Products **7** and **8** from the Reaction of CBN with the Diazonium Salt **5k**

The reaction between CBN and the diazonium salt prepared from *para*-nitroaniline was conducted in an ethanolic solution of NaOH using the same method as that used for CBD, yielding a purple mixture. TLC indicated that the spot corresponding to CBN diminished after 15 min, with several new spots appearing. These were separated by silica gel column chromatography; the main orange spot exhibited an R_f value of 0.13 (hexane/ethyl acetate = 10/1) as compound **7**, and another brown spot showed an R_f value of 0.50 (hexane/ethyl acetate = 10/1) as compound **8**. The ^1H NMR spectra of **7** and **8** each showed 29 proton signals, and the integration results indicated that they were produced by the reaction of CBN with one equivalent of *para*-nitroaniline. Figure 3 presents the key HMBC correlations for the isolated compound **7**. In compound **7**, a hydrogen-bonded signal was observed at 12.11 ppm in the ^1H NMR spectrum, and a peak characteristic of conjugated carbonyl carbons was observed at 184.5 ppm in the ^{13}C NMR spectrum. This trend is the same as that of quinoneimine **2**, the product of the reaction between CBN and Fast Blue RR, as reported previously [13]. HMBC correlations of **7** were observed between the proton signal at 12.11 ppm and the carbon peaks at 147.5 and 114.5 ppm, which were attributed to the benzene ring of *para*-nitroaniline (Figure 3a), and a NOESY correlation was observed between the proton signal at 12.11 ppm and the methyl signal of the pyran ring (Figure 3b). This suggests that compound **7** was in the quinoneimine form and that *para*-nitroaniline was bonded to the *para* position of the original phenol. Compound **7** was isolated in 58% yield.

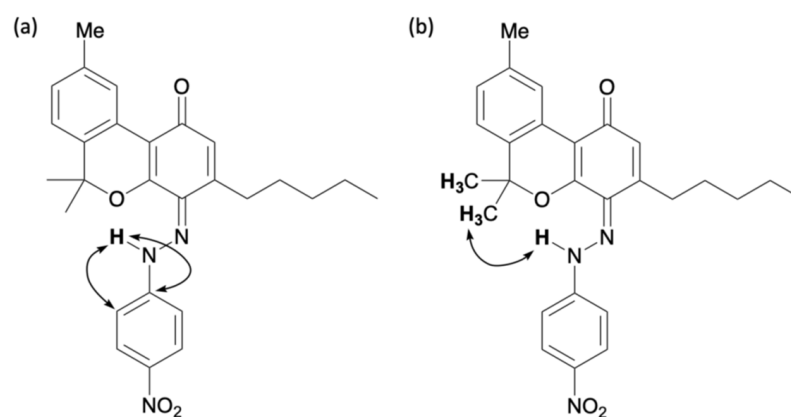


Figure 3. Key correlations for 7: (a) HMBC and (b) NOESY.

Compound **8** showed a proton signal at 16.92 ppm, corresponding to a hydrogen-bonded proton attached to either oxygen or nitrogen atom, which was downfield from that of compound **7**. ^{13}C NMR showed a signal at 169.5 ppm, slightly upfield from the quinoneimine carbon and slightly downfield from the phenolic carbon. HMBC of **8** showed a correlation from the proton signal at 16.92 to the carbon signal at 150.3 ppm, which was attributed to *para*-nitroaniline, indicating that the proton 16.92 ppm signal was not a phenolic hydrogen but a hydrogen bonded to a nitrogen atom of quinoneimine. Furthermore, HMBC correlations were observed between the 133.3 ppm carbon signal corresponding to the benzene ring of CBN and the 16.92 ppm proton signal, as well as the 2.88 ppm proton signal corresponding to the proton on the methylene portion of the pentyl group of CBN (Figure 4). These results indicated that **8** was a quinoneimine, in which *para*-nitroaniline was bound to the phenol moiety of CBN. As this differed from the measurement results for compound **7**, for which *para*-nitroaniline is bound to the *para* position of the original phenol, it can be concluded that compound **8** was bound to the *ortho*-position. Compound **8** was isolated in 20% yield, and the ratio of **7**:**8** was approximately 3:1. Other spots observed by TLC were likely due to unreacted CBN and decomposed products. The proposed formation mechanisms of **7** and **8** are shown in Scheme 2; it involves the addition of a diazonium salt to the *para*- or *ortho*-position, followed by tautomerization to the imine (instead of rearomatization as in the case of **6**).

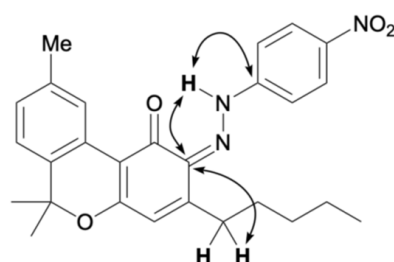
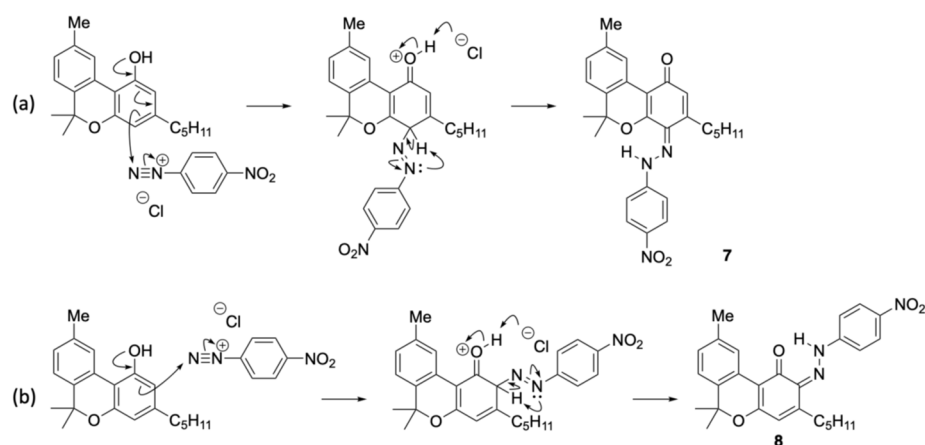


Figure 4. Key HMBC correlations for **8**.

In general, orthoquinones are more unstable and difficult to produce than paraquinones; therefore, **7** was the main product. Although orthoquinones are generally either not produced or are produced in such small amounts that they cannot be isolated, in this reaction, orthoquinone **8** was produced and isolated, which was attributed to the high reactivity of the diazonium salt prepared from *para*-nitroaniline.



Scheme 2. Proposed formation mechanisms of (a) 7 and (b) 8.

2.2.3. Colored Products 9 and 10 from the Reaction of Δ^9 -THC with the Diazonium Salt 5k

The reaction between Δ^9 -THC and the diazonium salt prepared from *para*-nitroaniline was conducted in an ethanol solution of NaOH, as described above, yielding a red reaction mixture. After 15 min, the spot corresponding to Δ^9 -THC almost completely disappeared, and several new spots were observed by TLC (Figure 5). The small spots with high polarity were assumed to correspond to decomposition products because of the basic conditions. The two main spots were separated by silica gel column chromatography; the main yellow spot, corresponding to 9, exhibited an R_f value of 0.14 (hexane/ethyl acetate = 5/1), and a red spot, assigned to 10, had an R_f value of 0.71. Figure 6 shows the results of the analysis of the isolated compound 9. The ¹H NMR spectrum of 9 showed 33 proton signals. The integration results confirmed that 9 was the product formed by the reaction of Δ^9 -THC with one equivalent of *para*-nitroaniline. Furthermore, a signal at 12.04 ppm was observed in the ¹H NMR spectrum of 9. This corresponds to a proton on an oxygen or nitrogen atom, similar to the downfield proton signal observed in *para*-quinoneimines 2, 3, and 7. Furthermore, the ¹³C NMR spectrum showed a peak at 185.6 ppm characteristic of the conjugated carbonyl carbon. HMBC correlations were observed between the 12.04 ppm proton signal and the 147.8 and 113.6 ppm carbon signals assigned to the benzene rings of *para*-nitroaniline (Figure 6a). In addition, NOESY correlations were observed between the 12.21 ppm proton signal and the signals of the methyl groups on the dimethyl pyran ring (Figure 6b). These results suggested that compound 9 was a *para*-quinoneimine, such as compounds 2, 3, and 7, and contained a *para*-nitroaniline moiety bonded to the *para* position of the original phenol group of Δ^9 -THC. Compound 9 was isolated in 30% yield.

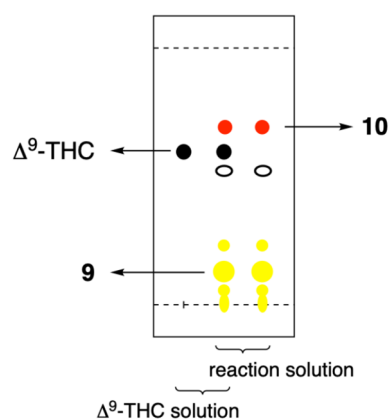


Figure 5. TLC profile of the reaction of Δ^9 -THC with the diazonium salt 5k after 15 min (hexane/ethyl acetate = 5/1).

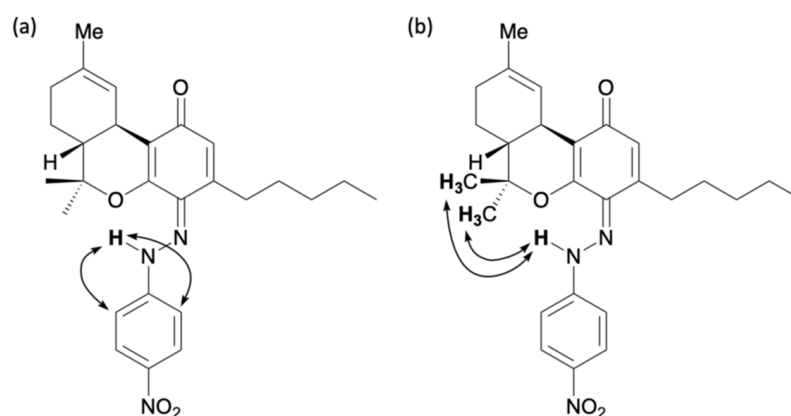


Figure 6. Key correlations for **9**: (a) HMBC and (b) NOESY.

The ^1H NMR spectrum of compound **10** showed 33 proton signals, and based on integration results, it was determined to be the reaction product of Δ^9 -THC with one equivalent of *para*-nitroaniline, similar to compound **9**. However, unlike compound **9**, a proton signal at 16.64 ppm and a carbon signal at 172.5 ppm were observed for compound **10**. This is similar to the *ortho*-quinoneimine **8**. HMBC correlations were observed between the 16.64 ppm proton signal and the carbon signals at 150.1 and 117.8 ppm, which were assigned to the benzene rings of *para*-nitroaniline. This revealed that compound **10** was present in the quinoneimine form rather than the azo form. In addition, a carbon signal at 133.1 ppm corresponding to the benzene ring of Δ^9 -THC was correlated with a signal at 16.64 ppm corresponding to a proton on a nitrogen atom, and a signal at 2.19–2.17 ppm corresponding to the methylene portion of the pentyl group of Δ^9 -THC (Figure 7). These results suggest that compound **10** was *ortho*-quinoneimine, like compound **8**, containing a *para*-nitroaniline moiety bonded to the *ortho*-position of the original phenol group of Δ^9 -THC. Compound **10** was isolated in 10% yield, and the ratio of **9**:**10** was approximately 3:1. This was the same as the reaction between CBN and the diazonium salt prepared from *para*-nitroaniline, but with a lower yield. The low yield was because some decomposed products were also detected due to the instability of Δ^9 -THC.

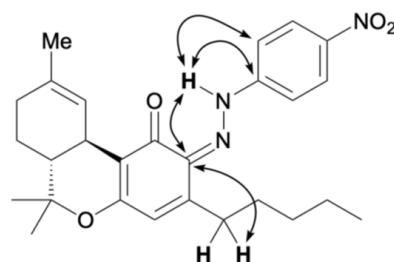


Figure 7. Key HMBC correlations for **10**.

Figure 8 shows the UV-vis spectra of 50 μM ethanol solutions of **6**–**10**. The maximum absorption wavelengths were 448 nm for azo compound **6** from CBD, 425 nm for *para*-quinoneimine **7** from CBN, 420 nm for *ortho*-quinoneimine **8** from CBN, 440 nm for *para*-quinoneimine **9** from Δ^9 -THC, and 430 nm for *ortho*-quinoneimine **10** from Δ^9 -THC. Interestingly, *para*-quinoneimine exhibited higher intensity than *ortho*-quinoneimine despite being at the same concentration.

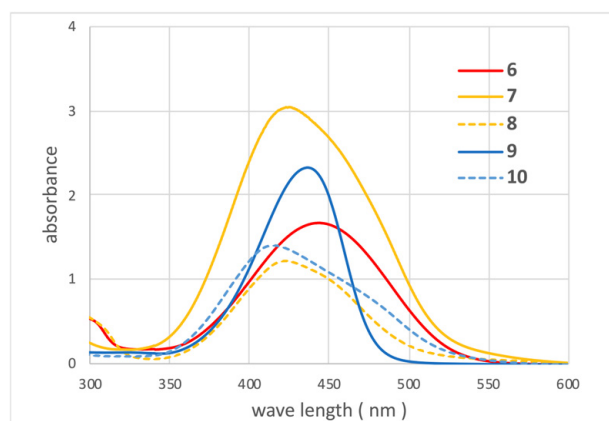


Figure 8. UV-vis spectra of **6** (red), **7** (yellow), **8** (dotted yellow), **9** (blue), and **10** (dotted blue).

2.2.4. Colored Product **11** from the Reaction of CBG with the Diazonium Salt **5k**

The reaction between CBG and the diazonium salt prepared from *para*-nitroaniline was performed in an ethanol solution of NaOH according to the aforementioned method, yielding a brown reaction mixture. After 15 min, the spot corresponding to CBG almost completely disappeared, and new spots were observed by TLC. Product **11** corresponded to a brown spot with an R_f value of 0.75 (hexane/dichloromethane = 4/1) and was subsequently isolated by silica gel chromatography. The ^1H NMR spectrum of **11** exhibited 35 proton signals, and the integration values indicated that **11** was formed from CBG and one equivalent of *para*-nitroaniline. Figure 9 presents the key HMBC correlations for isolated compound **11**. A strong downfield resonance was observed at 15.70 ppm, which was similar to that of azo compounds **1** and **4**, the products of CBD and diazonium salts. HMBC correlation was observed between this proton signal and the carbon peaks at 163.3, 132.2, and 112.2 ppm, which were assigned to the benzene carbon of CBG; thus, the proton signal at 15.70 ppm corresponds to the proton of phenol, and compound **11** was determined to be in the azo form. Compound **11** was isolated in 83% yield without any disubstituted compounds.

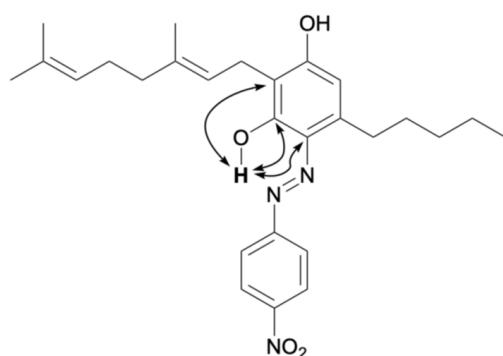


Figure 9. Key HMBC correlations for **11**.

2.2.5. Colored Products **12**–**15** from the Reaction of HHC with the Diazonium Salt **5k**

HHC was prepared by the hydrogenation of Δ^9 -THC, and a 1:1 mixture of two diastereomers, depending on the stereochemistry of the methyl group, was used. The reaction between HHC and the diazonium salt prepared from *para*-nitroaniline was carried out according to the aforementioned method, yielding a yellow reaction mixture. After 15 min, the spot corresponding to HHC almost completely disappeared, and multiple new spots, including two major spots, were observed by TLC. The yellow spots with R_f values of 0.06 and 0.38 (hexane/dichloromethane = 2/1) were separated by silica gel column chromatography, and each was purified by PTLC to isolate compounds **12** and **13**

from the highly polar spot ($R_f = 0.06$), and compounds **14** and **15** from the less polar spot ($R_f = 0.38$). The ^1H NMR spectra of compounds **12**–**15** each showed 35 proton signals, and the integration results indicated that they were formed from HHC and one equivalent of *para*-nitroaniline.

A proton signal at 12.03 ppm and a carbon signal at 185.8 ppm were observed for compound **12**. This is similar to the *para*-quinoneimine-type compounds **2**, **3**, **7**, and **9**. HMBC correlations were observed between the 12.03 ppm proton signal and the carbon signals at 148.3 and 113.5 ppm, which were assigned to the benzene rings of *para*-nitroaniline (Figure 10). Although no correlation with dimethyl groups were observed in the ROESY spectrum, based on previous results, compound **12** was suggested to be *para*-quinoneimine. For compound **13**, which is the 9-methyl epimer of compound **12**, a proton signal was observed at 12.04 ppm, and a carbon signal at 185.9 ppm, and similar HMBC and ROESY correlations showed that compound **13** was also *para*-quinoneimine. The isolated yields of **12** and **13** were 17% and 29%, respectively. Due to severe peak overlap, the stereochemistry of the 9-position (methyl group) could not be elucidated in CDCl_3 ; however, based on previous reports [15], it was estimated that compound **13**, whose 10α position was observed in a high magnetic field, was the *R*-configuration and **12** the *S*-configuration.

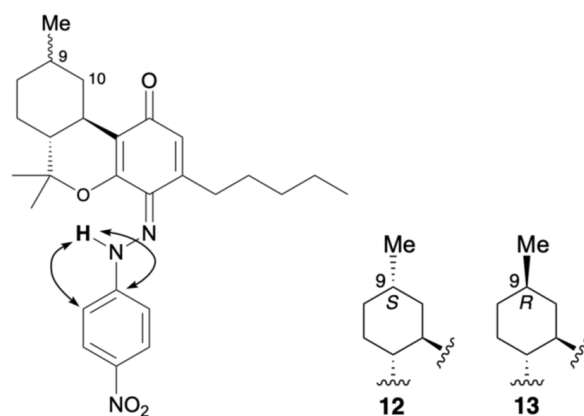


Figure 10. Key HMBC correlations for **12** and **13**.

In compound **14**, a proton signal was observed at 16.56 ppm, which is quite low-field, and a carbon signal at 172.8 ppm, which is similar to the conjugated carbonyl carbon, and the *ortho*-quinoneimine-type compounds **8** and **10**. Figure 10 shows the analysis results for the isolated compound **14**. HMBC correlations were observed between the 16.56 ppm proton signal and the carbon signal at 150.2 ppm, which was assigned to the benzene rings of *para*-nitroaniline; thus, **14** is in the quinoneimine form (Figure 11). Although no HMBC correlation was identified between proton signals of the pentyl group and a carbon signal of imine carbon, based on previous results, compound **14** was suggested to be *ortho*-quinoneimine, like compounds **8** and **10**. In compound **15**, a proton signal was observed at 16.65 ppm and a carbon signal at 173.5 ppm, and along with similar HMBC correlations, it was concluded that compound **15** was also *ortho*-quinoneimine. The isolated yields of compounds **14** and **15** were 6% and 12%, respectively. The stereochemistry of the 9-position (methyl group) could also not be determined for these compounds; however, as mentioned above, it was estimated that compound **15**, whose 10α position was observed in a high magnetic field, was the *R*-configuration, and **14** the *S*-configuration. More detailed NMR analysis of **12**–**15**, e.g., changing the solvent, will continue in the future.

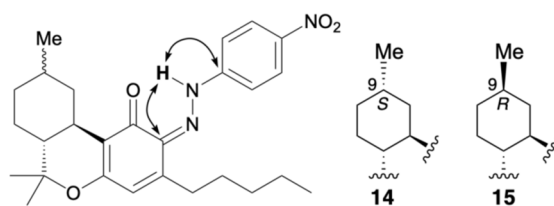


Figure 11. Key HMBC correlations for **14** and **15**.

The ratio of *para*-quinoneimine to *ortho*-quinoneimine was approximately 2.5:1. This is slightly different from that of CBN and Δ^9 -THC because of losses during diastereomer separation. Therefore, it was clear that the reaction of cannabinoids with a benzopyran structure that only have one phenol group with the diazonium salt **5k** tends to produce quinoneimine-type compounds with a *para:ortho* ratio of approximately 3:1.

2.2.6. Colored Product **16** from the Reaction of CBC with the Diazonium Salt **5k**

The reaction between CBC and the diazonium salt prepared from *para*-nitroaniline was carried out according to the aforementioned method, yielding a brown reaction mixture. After 15 min, the spot corresponding to CBC almost completely disappeared, and new spots were observed by TLC. Compound **16** corresponded to a brown spot with an R_f value of 0.75 (dichloromethane/hexane = 2/1) and was isolated by silica gel column chromatography. The ^1H NMR spectrum of compound **16** showed 33 proton signals, and the integrated values indicated that it was formed from CBC and one equivalent of *para*-nitroaniline, as previously described. Based on previous findings, cannabinoids containing a pyran ring were thought to exist in the quinoneimine form, but for compound **16**, a carbon signal at 162.3 ppm, which is similar to that of phenol, was observed by ^{13}C NMR. Careful analysis of the HMBC correlation revealed that the proton signal at 15.76 ppm correlated with the carbon signals at 161.4, 132.5, and 107.8 ppm, which were assigned to the benzene ring of CBC (Figure 12a). This showed that the lowest field signal at 15.76 ppm corresponds to the phenolic hydrogen atom, and that compound **16** was in the azo form. The chemical shifts at 15.76 ppm indicated that this phenolic hydrogen atom formed hydrogen bonds; that is, the azo moiety must be in the *ortho* position of the original phenol group. Therefore, compound **16** is an azo compound in which the *para*-nitroaniline is bonded to the *ortho* position of the original phenol in the CBC.

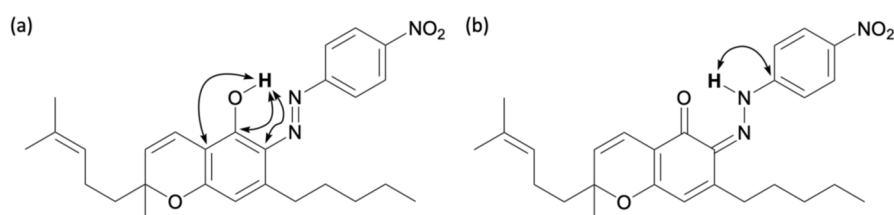


Figure 12. Key HMBC correlations for **16**: (a) azo form and (b) quinoneimine form.

Interestingly, weak HMBC correlations were also observed from a proton signal at 15.76 ppm to the carbon signal 151.9 ppm, corresponding to the benzene ring of *para*-nitroaniline (Figure 12b). This correlation is characteristic of quinoneimines. Here, the chemical shift at 161.4 ppm, corresponding to the carbon atom of the benzene ring bonded to phenol, was slightly lower in field than that of typical phenols and higher than that of quinoneimines. This suggests that compound **16** is an intermediate between phenols and quinoneimines with characteristics similar to those of phenols. That is, compound **16** is an azo compound with a small quinoneimine contribution. The reason why **16** was the main product is unclear; however, it is speculated that **16** is a thermodynamically stable compound with contributions from both the azo and quinoneimine forms, and that

the prenyl group attached to the pyran ring in CBC imposes steric hindrance during the reaction at the *para*-position. Further detailed analysis of this reactivity will be performed using computational chemistry and other methods in the future.

2.2.7. Reaction of Δ^9 -THC-O with the Diazonium Salt **5k**

The reaction between Δ^9 -THC-O and the diazonium salt prepared from *para*-nitroaniline was performed according to the aforementioned method, yielding a red reaction mixture. After 15 min, multiple new spots were observed by TLC. Of these, 58% of the initial Δ^9 -THC-O was recovered. In addition, compounds **9** and **10** were obtained in 6% and 1% yields, respectively. In compounds **9** and **10**, the acetyl groups have been removed. Therefore, the reaction did not proceed in the absence of free phenol. This is consistent with the fact that there was nearly no color change when Δ^9 -THC-O was added to the blank solution of the diazonium salt in Section 2.1. The slight coloration was due to the removal of the acetyl group to form Δ^9 -THC, which then reacted. The poor conversion was due to the decomposition caused by the instability of Δ^9 -THC-O, similar to Δ^9 -THC.

2.2.8. Reaction of HHC-O with the Diazonium Salt **5k**

HHC-O was prepared by the acetylation of HHC, a 1:1 mixture of two diastereomers, depending on the stereochemistry of the methyl group. The reaction between HHC-O and the diazonium salt prepared from *para*-nitroaniline was performed according to the aforementioned method, yielding a red reaction mixture. After 15 min, multiple new spots were observed by TLC. Surprisingly, 64% of deacetylated HHC was obtained. In addition, compounds **12** and **13** were obtained in 8% yield, whereas compounds **14** and **15** were obtained in 6% yield. Deacetylation occurred due to the basic conditions of this reaction. When the acetyl group was removed and a free phenol was formed, which was expected to react with the diazonium salt, HHC was recovered. This could be because the pH of the reaction solution became slightly acidic due to the removal of the acetyl group, and the reaction was not basic enough to proceed. It is unclear why deacetylation hardly occurred in the Δ^9 -THC-O reaction of Section 2.2.7, but a slight difference in basicity might have had a large effect.

2.2.9. Colored Product **17** from the Reaction of CBDA with the Diazonium Salt **5k**

The reaction between CBDA and the diazonium salt prepared from *para*-nitroaniline was performed as described above, yielding a purple reaction mixture. After 15 min, the spot corresponding to CBDA almost completely disappeared, and multiple new spots were observed by TLC. The major yellow spot with an R_f value of 0.38 (hexane/ethyl acetate = 5/1) was isolated by silica gel column chromatography. This isolated compound showed analytical results identical to those of compound **6** and was obtained in 32% yield, indicating that decarboxylation had occurred. The diazonium salt was prepared under strongly acidic conditions, and the direct addition of CBDA to this solution caused decarboxylation to form CBD, which then reacted with the diazonium salt. Therefore, after preparing the diazonium salt, the solution became basic before adding CBDA. TLC analysis confirmed the appearance of multiple new spots. The three major spots were identified and separated using silica gel column chromatography. One spot was the starting CBDA, which was recovered in 50% yield. The second spot was compound **6**, which was obtained in 10% yield. The third new spot was a yellow spot with an R_f value of 0.13 (hexane/ethyl acetate = 6/1). The ^1H NMR spectrum of **17** showed 31 proton signals, excluding those originating from one hydroxy group and the carbonyl group, and the integration values indicated that they were formed from CBDA and one equivalent of *para*-nitroaniline. Furthermore, the ^{13}C NMR spectrum of compound **17** showed 28 carbons with a carbonyl peak at 175.0 ppm, indicating that decarboxylation did not occur. Signals were observed at

15.70 ppm in the ^1H NMR spectrum and 166.7 ppm in the ^{13}C NMR spectrum, which were similar to those observed for azo compounds **1**, **4**, and **11**, i.e., the products from CBD and CBG. Therefore, **17** was proposed to be an azo compound (Figure 13). However, because no hydroxyl group signals or HMBC correlations were observed in deuterated chloroform, it cannot be completely ruled out that **17** was *ortho*-quinoneimine. Further detailed NMR analysis of **17**, e.g., changing the solvent, such as **12–15**, will continue in the future. The isolated yield of compound **17** was 18%. The low yield of this product was attributed to a decrease in the electron density of the benzene ring caused by the carboxyl group.

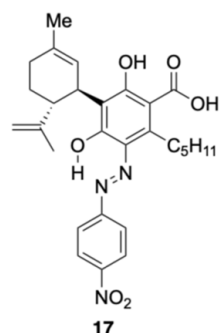


Figure 13. Proposed structure of **17**.

3. Materials and Methods

3.1. Materials

CBD powder was purchased from CannaTech Co., Ltd. (Kanagawa, Japan), and CBN and CBG powders were purchased from Leep Co., Ltd. (Tokyo, Japan). All the compounds were used as received. Δ^9 -THC was synthesized from CBD using a previously reported method [16], and the NMR data for the synthesized Δ^9 -THC were matched using a previous report [17]. HHC was synthesized from Δ^9 -THC by standard reduction, and NMR data for the synthesized HHC were matched using a previous report [15]. CBC was synthesized using a previously reported method, and the NMR data for the synthesized CBC were matched using a previous report [18]. Δ^9 -THC-O and HHC-O were synthesized from Δ^9 -THC and HHC, respectively, via standard acetylation. CBDA was synthesized from CBD using a previously reported method [19], and the NMR data for the synthesized CBDA were matched using a previous report [17]. Other reagents were purchased from commercial suppliers and used as received.

3.2. General Synthesis and Analysis Information

The reaction mixtures were magnetically stirred and monitored by TLC using pre-coated silica gel plates. Column chromatography was performed using silica gel (60 μm). ^1H (400 MHz) and ^{13}C (100 MHz) NMR spectra were recorded on a JNM-ECZ400S NMR spectrometer, and ^1H (500 MHz) and ^{13}C (125 MHz) NMR spectra were recorded on a JNM-ECZL500R NMR spectrometer (JEOL Ltd., Tokyo, Japan) at 296 K, unless otherwise stated. Chemical shifts are given in parts per million (ppm) downfield from that of tetramethylsilane as an internal standard (0.00 ppm), and coupling constants (J) are reported in Hz. The splitting patterns are abbreviated as singlet (s), doublet (d), triplet (t), multiplet (m), and broad (br). High-resolution mass spectra (HRMS) were recorded using an X500R QTOF electrospray ionization time-of-flight mass spectrometer (AB Sciex LLC, Marlborough, MA, USA). IR spectra were recorded on a Spectrum 100 FT-IR spectrometer equipped with an ATR (diamond) accessory (PerkinElmer Inc., Waltham, MA, USA). UV-vis spectra were obtained using ethanol solutions of the samples (50 μM) and recorded on a V-750 Spectrophotometer (JASCO Corporation, Tokyo, Japan).

3.3. General Methods

3.3.1. Color Reactions

NaNO₂ (1 equiv) was added to a stirred solution of aniline (1 equiv) in 4 N aqueous HCl (0.1 M) at 0 °C. After stirring for 30 min, to 50 µL of this diazonium salt solution, 100 mM cannabinoid in EtOH (20 µL) and EtOH (40 µL) was added at 23 °C, and the solution was shaken and the color monitored.

3.3.2. Isolation of Compounds 6–16

NaNO₂ (1 equiv) was added to a stirred solution of *para*-nitroaniline (1 equiv) in 3 N aqueous HCl (0.1 M) at 0 °C. After stirring for 30 min, cannabinoid (1 equiv) in EtOH (0.05 M) was added at 23 °C, followed by 10 N aqueous NaOH (60 equiv). The mixture was stirred for 15 min, after which half the volume of the solvent was removed in vacuo and water was added. The crude product was extracted with ethyl acetate (×3), and the combined organic extracts were washed with brine, dried over Na₂SO₄, and concentrated in vacuo. The residue was purified by column chromatography (hexane/ethyl acetate or hexane/dichloromethane) to obtain products 6–16.

3.3.3. Isolation of Compound 17

NaNO₂ (28.7 mg, 0.416 mmol, 1 equiv) was added to a stirred solution of *para*-nitroaniline (57.5 mg, 0.416 mmol, 1 equiv) in 3 N aqueous HCl (10 mL, 0.1 M) at 0 °C. After stirring for 30 min, the reaction mixture was adjusted to pH 7 by adding 10 N aqueous NaOH (2.4 mL), followed by the addition of 0.05 M CBDA (149.2 mg, 0.416 mmol, 1 equiv) in EtOH (8 mL) at 23 °C. The mixture was stirred for 15 min, after which half the volume of the solvent was removed in vacuo and water was added. The crude product was extracted with ethyl acetate (×3), and the combined organic extracts were washed with brine, dried over Na₂SO₄, and concentrated in vacuo. The residue was purified using column chromatography (hexane/ethyl acetate = 6/1) to obtain product 17.

3.4. Spectral Data

2-[(1'*R*,6'*R*)-6'-Isopropenyl-3'-methylcyclohex-2-en-1-yl]-4-[(*E*)-(4-nitrophenyl)diazenyl]-5-pentylbenzene-1,3-diol (6): CBD (0.19 mmol scale), quantitative yield; purple solid; R_f 0.38 (hexane/ethyl acetate = 5/1); mp 45–48 °C; ¹H NMR (500 MHz, CDCl₃) δ 15.70 (s, 1H, OH), 8.33–8.31 (m, 2H), 7.76–7.74 (m, 2H), 6.93 (br, 1H, OH), 6.33 (s, 1H), 5.57 (s, 1H), 4.56 (s, 1H), 4.48 (s, 1H), 4.06 (s, 1H), 2.95–2.90 (m, 1H), 2.86–2.80 (m, 1H), 2.36 (s, 1H), 2.27–2.20 (m, 1H), 2.14–2.10 (m, 1H), 1.81 (s, 5H), 1.74 (s, 3H), 1.69–1.63 (m, 2H), 1.38–1.35 (m, 4H), 0.90 (t, 3H, *J* = 7.1 Hz); ¹³C NMR (125 MHz, CDCl₃) δ 164.6, 152.0, 146.9, 146.1, 132.0, 125.3, 123.5, 119.7, 115.6, 113.4, 111.5, 46.7, 34.4, 31.8, 31.5, 30.8, 30.1, 27.6, 23.8, 22.5, 19.0, 14.1 (several signals overlapped); IR (ATR) 3368, 3072, 2924, 1588, 1398, 1252; HRMS (ESI) *m/z* calcd. for C₂₇H₃₄N₃O₄: 464.2544 (M + H⁺), found: 464.2544.

(*Z*)-6,6,9-Trimethyl-4-[2-(4-nitrophenyl)hydrazineylidene]-3-pentyl-4,6-dihydro-1*H*-benzo[*c*]chromen-1-one (7): CBN (0.19 mmol scale), 58% yield; orange solid; R_f 0.13 (hexane/ethyl acetate = 10/1); mp 130–132 °C; ¹H NMR (400 MHz, CDCl₃) δ 12.11 (s, 1H, NH), 8.43 (s, 1H), 8.29–8.27 (m, 2H), 7.29–7.28 (m, 1H), 7.26–7.25 (m, 1H), 7.15 (d, 1H, *J* = 8.7 Hz), 7.07 (d, 1H, *J* = 7.9 Hz), 6.35 (s, 1H), 2.70 (t, 2H, *J* = 7.5 Hz), 2.39 (s, 3H), 1.82 (s, 6H), 1.69–1.64 (m, 2H), 1.43–1.37 (m, 4H), 0.93 (t, 3H, *J* = 7.0 Hz); ¹³C NMR (100 MHz, CDCl₃) δ 184.5, 152.7, 148.5, 147.5, 142.9, 138.0, 133.1, 130.6, 129.4, 127.7, 126.9, 126.1, 125.2, 121.6, 114.5, 113.9, 82.2, 31.9, 31.5, 29.3, 27.7, 22.5, 21.5, 14.1 (several signals overlapped); IR (ATR) 3030, 2947, 2908, 1592, 1444, 1394; HRMS (ESI) *m/z* calcd. for C₂₇H₃₀N₃O₄: 460.2236 (M + H⁺), found: 460.2231.

(Z)-6,6,9-Trimethyl-2-[2-(4-nitrophenyl)hydrazineylidene]-3-pentyl-2,6-dihydro-1H-benzo[c]chromen-1-one (**8**): 20% yield; brown solid; R_f 0.50 (hexane/ethyl acetate = 10/1); mp 63–65 °C; ^1H NMR (400 MHz, CDCl_3) δ 16.92 (s, 1H, NH), 8.56 (s, 1H), 8.36–8.33 (m, 2H), 7.76–7.72 (m, 2H), 7.10 (d, 2H, $J = 1.1$ Hz), 6.42 (s, 1H), 2.88 (t, 2H, $J = 7.7$ Hz), 2.42 (s, 3H), 1.74–1.68 (m, 2H), 1.67 (s, 6H), 1.45–1.35 (m, 4H), 0.99 (t, 3H, $J = 7.1$ Hz); ^{13}C NMR (100 MHz, CDCl_3) δ 169.5, 163.4, 150.3, 148.2, 145.5, 137.3, 133.9, 133.3, 128.1, 126.3, 126.0, 125.5, 122.3, 118.5, 115.1, 109.6, 80.2, 31.8, 31.5, 30.3, 27.8, 27.1, 22.5, 21.6, 14.1 (several signals overlapped); IR (ATR) 3301, 3077, 1634, 1608, 1458, 1424; HRMS (ESI) m/z calcd. for $\text{C}_{27}\text{H}_{28}\text{N}_3\text{O}_4$: 458.2085 (M-H^-), found: 458.2085.

(Z)-(6aR,10aR)-6,6,9-Trimethyl-4-[2-(4-nitrophenyl)hydrazineylidene]-3-pentyl-4,6,6a,7,8,10a-hexahydro-1H-benzo[c]chromen-1-one (**9**): THC (50 μmol scale), 30% yield; red solid; R_f 0.14 (hexane/ethyl acetate = 5/1); mp 76–79 °C; ^1H NMR (400 MHz, CDCl_3) δ 12.04 (s, 1H, NH), 8.27–8.25 (m, 2H), 7.31–7.20 (m, 2H), 6.25 (s, 1H), 6.13 (t, 1H, $J = 1.5$ Hz), 3.11 (d, 1H, $J = 15.3$ Hz), 2.72–2.57 (m, 2H), 2.19–2.17 (m, 2H), 1.92–1.89 (m, 1H), 1.74 (t, 1H, $J = 12.7$ Hz), 1.66 (s, 6H), 1.65–1.61 (m, 2H), 1.39–1.36 (m, 5H), 1.27 (s, 3H), 0.92 (t, 3H, $J = 7.1$ Hz); ^{13}C NMR (100 MHz, CDCl_3) δ 185.6, 153.9, 148.7, 147.8, 142.6, 134.1, 130.9, 126.2, 126.0, 122.5, 116.9, 113.6, 83.0, 44.9, 32.8, 31.8, 31.6, 31.1, 29.5, 27.7, 24.5, 23.2, 22.5, 20.0, 14.1; IR (ATR) 3283, 2927, 1628, 1594, 1426, 1402; HRMS (ESI) m/z calcd. for $\text{C}_{27}\text{H}_{34}\text{N}_3\text{O}_4$: 464.2544 ($\text{M} + \text{H}^+$), found: 464.2542.

(Z)-(6aR,10aR)-6,6,9-Trimethyl-2-[2-(4-nitrophenyl)hydrazineylidene]-3-pentyl-2,6,6a,7,8,10a-hexahydro-1H-benzo[c]chromen-1-one (**10**): 10% yield; red solid; R_f 0.71 (hexane/ethyl acetate = 5/1); mp 63–65 °C; ^1H NMR (400 MHz, CDCl_3) δ 16.64 (s, 1H, NH), 8.32–8.29 (m, 2H), 7.66–7.64 (m, 2H), 6.40 (t, 1H, $J = 1.5$ Hz), 6.23 (s, 1H), 3.17 (d, 1H, $J = 11.0$ Hz), 2.88–2.80 (m, 1H), 2.76–2.67 (m, 1H), 2.19–2.17 (m, 2H), 1.93–1.89 (m, 1H), 1.70 (s, 3H), 1.66–1.63 (m, 3H), 1.47 (s, 3H), 1.44–1.36 (m, 5H), 1.15 (s, 3H), 0.91 (t, 3H, $J = 7.1$ Hz); ^{13}C NMR (100 MHz, CDCl_3) δ 172.5, 163.7, 150.1, 145.8, 144.9, 134.1, 133.1, 125.5, 122.7, 117.8, 115.9, 111.2, 80.6, 45.4, 32.8, 31.8, 31.2, 31.2, 30.2, 27.2, 24.7, 23.3, 22.5, 20.0, 14.1; IR (ATR) 2926, 2856, 1726, 1591, 1491, 1385; HRMS (ESI) m/z calcd. for $\text{C}_{27}\text{H}_{32}\text{N}_3\text{O}_4$: 462.2398 (M-H^-), found: 462.2399.

2-[(E)-3,7-Dimethylocta-2,6-dien-1-yl]-4-[(E)-(4-nitrophenyl)diazanyl]-5-pentylbenzene-1,3-diol (**11**): CBG (0.19 mmol scale), 83% yield; brown solid; R_f 0.75 (hexane/dichloromethane = 4/1); mp 72–74 °C; ^1H NMR (400 MHz, CDCl_3) δ 15.70 (s, 1H, OH), 8.35–8.32 (m, 2H), 7.79–7.75 (m, 2H), 6.52 (br, 1H, OH), 6.36 (s, 1H), 5.32–5.29 (m, 1H), 5.06–5.03 (m, 1H), 3.41 (d, 2H, $J = 7.3$ Hz), 2.90 (t, 2H, $J = 7.6$ Hz), 2.14–2.07 (m, 4H), 1.81 (s, 3H), 1.68 (s, 3H), 1.66–1.60 (m, 2H), 1.57 (s, 3H), 1.40–1.35 (m, 4H), 0.90 (t, 3H, $J = 7.0$ Hz); ^{13}C NMR (100 MHz, CDCl_3) δ 163.3, 163.2, 152.2, 146.9, 146.3, 140.2, 132.2, 132.1, 125.3, 123.6, 121.0, 120.1, 112.5, 112.1, 39.7, 31.8, 31.5, 31.1, 26.2, 25.7, 22.5, 21.3, 17.7, 16.3, 14.1; IR (ATR) 3381, 2959, 2959, 1584, 1509, 1438, 1154; HRMS (ESI) m/z calcd. for $\text{C}_{27}\text{H}_{34}\text{N}_3\text{O}_4$: 464.2555 (M-H^-), found: 464.2554.

(Z)-(6aR,9S,10aR)-6,6,9-Trimethyl-4-[2-(4-nitrophenyl)hydrazineylidene]-3-pentyl-4,6,6a,7,8,9,10,10a-octahydro-1H-benzo[c]chromen-1-one (**12**): HHC (0.16 mmol scale), 17% yield; orange solid; R_f 0.38 (hexane/ethyl acetate = 6/1 \times 3); mp 88–91 °C; ^1H NMR (500 MHz, CDCl_3) δ 12.03 (s, 1H, NH), 8.26–8.24 (m, 2H), 7.21–7.19 (m, 2H), 6.20 (s, 1H), 2.83 (d, 1H, $J = 12.9$ Hz), 2.70–2.59 (m, 2H), 2.55 (t, 1H, $J = 12.8$ Hz), 2.13–2.10 (m, 1H), 1.67–1.62 (m, 7H), 1.60 (s, 3H), 1.51–1.46 (m, 1H), 1.40–1.36 (m, 4H), 1.26 (s, 3H), 1.14 (d, 3H, $J = 7.2$ Hz), 0.92 (t, 3H, $J = 14.2$ Hz); ^{13}C NMR (125 MHz, CDCl_3) δ 185.8, 154.0, 148.3, 147.9, 142.5, 131.0, 126.4, 126.0, 118.5, 113.5, 82.3, 49.0, 35.7, 32.1, 31.9, 31.5, 29.4, 27.7, 27.5, 22.5, 22.4, 19.7, 18.4, 14.1 (several signals overlapped); IR (ATR)

3420, 3282, 2926, 1722, 1594, 1402; HRMS (ESI) m/z calcd. for $C_{27}H_{36}N_3O_4$: 466.2700 ($M + H^+$), found: 466.2701.

(*Z*)-(6*aR*,9*R*,10*aR*)-6,6,9-Trimethyl-4-[2-(4-nitrophenyl)hydrazineylidene]-3-pentyl-4,6,6*a*,7,8,9,10,10*a*-octahydro-1*H*-benzo[*c*]chromen-1-one (**13**): 29% yield; orange solid; R_f 0.50 (hexane/ethyl acetate = 6/1 \times 3); mp 92–94 °C; 1H NMR (500 MHz, $CDCl_3$) δ 12.04 (s, 1H, NH), 8.26–8.25 (m, 2H), 7.22–7.20 (m, 2H), 6.20 (s, 1H), 2.98 (d, 1H, $J = 12.6$ Hz), 2.70–2.58 (m, 2H), 2.34 (t, 1H, $J = 12.5$ Hz), 1.90–1.82 (m, 2H), 1.66–1.61 (m, 6H), 1.47 (t, 1H, $J = 12.5$ Hz), 1.39–1.37 (m, 4H), 1.24 (s, 3H), 1.17–1.05 (m, 2H), 0.94–0.88 (m, 6H), 0.62 (q, 1H, $J = 11.8$ Hz); ^{13}C NMR (125 MHz, $CDCl_3$) δ 185.9, 153.7, 148.4, 147.9, 142.5, 130.9, 126.3, 126.0, 118.2, 113.6, 82.6, 48.2, 38.5, 35.3, 34.3, 32.5, 31.9, 31.5, 29.4, 27.8, 27.5, 22.5, 22.3, 19.6, 14.1; IR (ATR) 3419, 3282, 2922, 1723, 1594, 1402; HRMS (ESI) m/z calcd. for $C_{27}H_{36}N_3O_4$: 466.2700 ($M + H^+$), found: 466.2701.

(*Z*)-(6*aR*,9*S*,10*aR*)-6,6,9-Trimethyl-2-[2-(4-nitrophenyl)hydrazineylidene]-3-pentyl-2,6,6*a*,7,8,9,10,10*a*-octahydro-1*H*-benzo[*c*]chromen-1-one (**14**): 6% yield; orange solid; R_f 0.50 (hexane/ethyl acetate = 6/1 \times 2); mp 46–49 °C; 1H NMR (400 MHz, $CDCl_3$) δ 16.56 (s, 1H, NH), 8.31–8.28 (m, 2H), 7.66–7.62 (m, 2H), 6.21 (s, 1H), 3.05 (d, 1H, $J = 12.8$ Hz), 2.83–2.72 (m, 1H), 2.70–2.66 (m, 1H), 2.63 (t, 1H, $J = 13.1$ Hz), 2.50–2.47 (m, 1H), 2.18–2.08 (m, 2H), 1.67–1.63 (m, 6H), 1.41 (s, 3H), 1.38–1.36 (m, 6H), 1.20–1.17 (m, 4H), 0.92 (t, 3H, $J = 7.1$ Hz); ^{13}C NMR (100 MHz, $CDCl_3$) δ 172.8, 163.8, 150.2, 145.6, 144.8, 133.1, 125.5, 117.7, 115.9, 112.5, 80.1, 49.4, 35.3, 32.2, 31.9, 31.1, 30.1, 28.5, 27.6, 27.2, 22.7, 22.5, 19.7, 18.7, 14.1; IR (ATR) 2954, 2925, 1765, 1592, 1424, 1383; HRMS (ESI) m/z calcd. for $C_{27}H_{36}N_3O_4$: 466.2700 ($M + H^+$), found: 466.2707.

(*Z*)-(6*aR*,9*R*,10*aR*)-6,6,9-Trimethyl-2-[2-(4-nitrophenyl)hydrazineylidene]-3-pentyl-2,6,6*a*,7,8,9,10,10*a*-octahydro-1*H*-benzo[*c*]chromen-1-one (**15**): 12% yield; red solid; R_f 0.38 (hexane/ethyl acetate = 6/1 \times 2); mp 48–50 °C; 1H NMR (400 MHz, $CDCl_3$) δ 16.65 (s, 1H, NH), 8.31–8.28 (m, 2H), 7.64–7.60 (m, 2H), 6.21 (s, 1H), 3.19 (d, 1H, $J = 12.8$ Hz), 2.83–2.78 (m, 1H), 2.72–2.69 (m, 1H), 2.40 (t, 1H, $J = 12.5$ Hz), 1.89–1.81 (m, 2H), 1.71–1.61 (m, 3H), 1.57 (s, 2H), 1.43 (s, 3H), 1.41–1.36 (m, 5H), 1.13 (s, 3H), 0.96 (d, 3H, $J = 6.42$ Hz), 0.91 (t, 3H, $J = 7.1$ Hz), 0.67 (q, 1H, $J = 11.9$ Hz); ^{13}C NMR (100 MHz, $CDCl_3$) δ 173.5, 163.7, 150.0, 145.6, 144.8, 133.3, 125.5, 117.6, 116.0, 112.4, 80.3, 48.6, 38.3, 35.5, 34.4, 32.6, 31.9, 31.1, 30.1, 27.7, 27.4, 22.54, 22.50, 19.6, 14.0; IR (ATR) 2920, 2857, 1727, 1591, 1490, 1385; HRMS (ESI) m/z calcd. for $C_{27}H_{36}N_3O_4$: 466.2700 ($M + H^+$), found: 466.2700.

2-Methyl-2-(4-methylpent-3-en-1-yl)-6-[(*E*)-(4-nitrophenyl)diazenyl]-7-pentyl-2*H*-chromen-5-ol (**16**): CBC (0.33 mmol scale), 75% yield; brown solid R_f 0.75 (hexane/dichloromethane = 2/1); mp 62–65 °C; 1H NMR (400 MHz, $CDCl_3$) δ 15.76 (s, 1H, OH), 8.34–8.31 (m, 2H), 7.75–7.72 (m, 2H), 6.72 (d, 1H, $J = 10.2$ Hz), 6.32 (s, 1H), 5.46 (d, 1H, $J = 10.2$ Hz), 5.11–5.08 (m, 1H), 2.89 (t, 2H, $J = 7.7$ Hz), 2.10 (q, 2H, $J = 11.8$ Hz), 1.83–1.76 (m, 1H), 1.70–1.68 (m, 2H), 1.66 (s, 3H), 1.65–1.63 (m, 1H), 1.58 (s, 3H), 1.45 (s, 3H), 1.40–1.34 (m, 4H), 0.91 (t, 3H, $J = 7.0$ Hz); ^{13}C NMR (100 MHz, $CDCl_3$) δ 162.3, 161.4, 151.9, 148.8, 146.2, 132.5, 132.0, 125.3, 125.1, 123.6, 119.6, 115.8, 112.7, 107.8, 81.6, 41.8, 31.8, 30.9, 25.7, 22.6, 22.5, 14.0 (several signals overlapped); IR (ATR) 3105, 2960, 1913, 1589, 1401, 1376; HRMS (ESI) m/z calcd. for $C_{27}H_{34}N_3O_4$: 464.2544 ($M + H^+$), found: 464.2544.

2,4-Dihydroxy-3-[(1'*R*,6'*R*)-6'-isopropenyl-3'-methylcyclohex-2-en-1-yl]-5-[(*E*)-(4-nitrophenyl)diazenyl]-6-pentylbenzoic acid (**17**): CBDA (0.41 mmol scale), 18% yield; orange solid R_f 0.13 (hexane/ethyl acetate = 6/1); mp 76–78 °C; 1H NMR (500 MHz, $CDCl_3$) δ 15.22 (br, 1H, OH), 8.39–8.33 (m, 2H), 7.88–7.86 (m, 2H), 5.25 (s, 1H), 4.53 (s, 1H), 4.49 (s, 1H), 4.14–4.11 (m, 1H), 3.57–3.45 (brm, 2H), 3.12–3.06 (m, 1H), 2.31–2.25 (m, 1H), 2.06–2.01 (m, 1H), 1.84–1.74 (m, 2H), 1.71 (s, 3H), 1.67–1.62 (m, 5H), 1.41–1.32

(m, 4H), 0.87 (t, 3H, $J = 7.0$ Hz) (one OH and the COOH was not observed); ^{13}C NMR (125 MHz, CDCl_3) δ 175.1, 166.7, 153.7, 152.3, 148.8, 147.6, 130.9, 126.4, 125.1, 124.3, 121.9, 117.2, 115.5, 113.4, 110.3, 44.1, 35.3, 32.5, 32.4, 30.5, 29.5, 29.3, 23.5, 22.4, 19.0, 14.1; IR (ATR) 2921, 2852, 1584, 1520, 1457, 1375; HRMS (ESI) m/z calcd. for $\text{C}_{28}\text{H}_{32}\text{N}_3\text{O}_6$: 506.2297 (M-H⁻), found: 506.2297.

4. Conclusions

We investigated a color diazo-coupling reaction for the detection of cannabis. Using the diazonium salt of *para*-nitroaniline, the reaction products were isolated and their structures determined by NMR analysis. CBD, CBG, CBC, and CBDA yielded the monosubstituted azo compounds **6**, **11**, **16**, and **17**, respectively. In particular, it was revealed for the first time that CBC reacts selectively at the *ortho*-position of the phenol, and the resulting compound **16** was also an azo compound with *ortho*-quinoneimine characteristics. Further investigation of this reaction will be carried out. The reaction products of CBN, Δ^9 -THC, and HHC were quinoneimines. A compound that reacted at the *para*-position of the original phenol and a positional isomer that reacted at the *ortho*-position were isolated in a *para:ortho* ratio of approximately 3:1. This is the first report of isolating two compounds, determining their structures, and calculating their yields and ratio for cannabinoids. The reaction did not proceed with compounds with protected hydroxyl groups, such as Δ^9 -THCO and HHCO, indicating that free phenols are required for the reaction with the diazonium salt. These findings are important for color reactions using diazonium salts, and they provide guidance for the development of highly sensitive reagents.

Supplementary Materials: The following supporting information can be downloaded from <https://www.mdpi.com/article/10.3390/molecules31050796/s1>. Figures S1–S6: NMR spectra of compound **6** (^1H , ^{13}C , COSY, HSQC, HMBC, ROESY); Figures S7–S12: NMR spectra of compound **7** (^1H , ^{13}C , COSY, HSQC, HMBC, NOESY); Figures S13–S18: NMR spectra of compound **8** (^1H , ^{13}C , COSY, HSQC, HMBC, NOESY); Figures S19–S24: NMR spectra of compound **9** (^1H , ^{13}C , COSY, HSQC, HMBC, NOESY); Figures S25–S30: NMR spectra of compound **10** (^1H , ^{13}C , COSY, HSQC, HMBC, NOESY); Figures S31–S36: NMR spectra of compound **11** (^1H , ^{13}C , COSY, HSQC, HMBC, NOESY); Figures S37–S42: NMR spectra of compound **12** (^1H , ^{13}C , COSY, HSQC, HMBC, ROESY); Figures S43–S48: NMR spectra of compound **13** (^1H , ^{13}C , COSY, HSQC, HMBC, ROESY); Figures S49–S54: NMR spectra of compound **14** (^1H , ^{13}C , COSY, HSQC, HMBC, NOESY); Figures S55–S60: NMR spectra of compound **15** (^1H , ^{13}C , COSY, HSQC, HMBC, NOESY); Figures S61–S66: NMR spectra of compound **16** (^1H , ^{13}C , COSY, HSQC, HMBC, NOESY); Figures S67–S72: NMR spectra of compound **17** (^1H , ^{13}C , COSY, HSQC, HMBC, NOESY).

Author Contributions: Conceptualization, K.N. and H.T.; methodology, K.N. and H.T.; investigation, H.N., K.N., R.A. and R.H.; writing—original draft preparation, H.N. and K.N.; writing—review and editing, H.A., A.I., M.T., K.H., A.S. and H.T.; project administration, H.T.; funding acquisition, H.A. All authors have read and agreed to the published version of the manuscript.

Funding: This research was funded by A-STEP (JPMJTR224B) from the Japan Science and Technology Agency.

Institutional Review Board Statement: Not applicable.

Informed Consent Statement: Not applicable.

Data Availability Statement: The original contributions presented in this study are included in the article/Supplementary Material. Further inquiries can be directed to the corresponding authors.

Conflicts of Interest: Author Hiroko Abe was employed by the company BioDesign Inc. The remaining authors declare that the research was conducted in the absence of any commercial or financial relationships that could be construed as a potential conflict of interest.

References

1. Hanus, L.O. Pharmacological and therapeutic secrets of plant and brain (endo)cannabinoids. *Med. Res. Rev.* **2009**, *29*, 213–271. [[CrossRef](#)] [[PubMed](#)]
2. Rock, E.M.; Parker, L.A. Constituents of *Cannabis sativa*. In *Cannabinoids and Neuropsychiatric Disorders*; Murillo-Rodriguez, E., Pandi-Perumal, S.R., Monti, J.M., Eds.; Springer Nature: Berlin/Heidelberg, Germany, 2020; pp. 1–13. Available online: https://link.springer.com/chapter/10.1007/978-3-030-57369-0_1#citeas (accessed on 24 January 2026).
3. Ministry of Health, Labour and Welfare. Available online: <https://www.mhlw.go.jp/content/11120000/001540416.pdf> (accessed on 22 December 2025).
4. Watanabe, K.; Yamaori, S.; Yamamoto, I. A study on the culture and sciences of the cannabis and marihuana XXIV. *Bol. Hokuriku Univ.* **2013**, *37*, 27–35.
5. Balfour, A. *Fourth Report of the Wellcome Tropical Research Laboratories at the Gordon Memorial College, Khartoum*; Baillière, Tindall & Cox: London, UK, 1911.
6. Ghamrawy, M.A. The detection of *Cannabis indica*. A new test. *J. Egypt. Med. Assoc.* **1937**, *20*, 193–208.
7. Duquenois, P.; Moustapha, H.N. Identification and assay of *Cannabis indica*. *J. Egypt. Med. Assoc.* **1938**, *21*, 224–227.
8. Korte, F.; Sieper, H. Zur chemischen Klassifizierung von Pflanzen XXIV. Untersuchung von Haschisch-Inhaltsstoffen durch Dünnschichtchromatographie. *J. Chromatogr.* **1964**, *13*, 90–98. [[CrossRef](#)] [[PubMed](#)]
9. Tsui, P.T.; Kelly, K.A.; Ponpipom, M.M.; Strahilevitz, M.; Sehon, A.H. Δ^9 -Tetrahydrocannabinol–Protein Conjugates. *Can. J. Biochem.* **1974**, *52*, 252–258. [[CrossRef](#)] [[PubMed](#)]
10. Chia, D.T.; Fike, S.A.; Nelson, J.T. Identification of the Reaction Product of Δ^8 -Tetrahydrocannabinol with KN Reagent. *J. Forens. Sci. Soc.* **1974**, *14*, 197–200. [[CrossRef](#)] [[PubMed](#)]
11. Luo, Y.R.; Han, J.; Yun, C.; Lynch, K.L. Azo Coupling-Based Derivatization Method for High-Selectivity Liquid Chromatography-Tandem Mass Spectrometry Analysis of Tetrahydrocannabinol and Other Aromatic Compounds. *J. Chromatogr. A* **2019**, *1597*, 109–118. [[CrossRef](#)] [[PubMed](#)]
12. França, H.S.; Acosta, A.; Jamal, A.; Romao, W.; Mulloor, J.; Almirall, J.R. Experimental and ab initio investigation of the products of reaction from Δ^9 -tetrahydrocannabinol (Δ^9 -THC) and the fast blue BB spot reagent in presumptive drug tests for cannabinoids. *Forensic Chem.* **2020**, *17*, 100212. [[CrossRef](#)]
13. Nakamura, K.; Nishiguchi, H.; Arai, R.; Hamajima, R.; Abe, H.; Ishida, A.; Tokeshi, M.; Higashi, K.; Saitoh, A.; Takahashi, H. Isolating and determining the structures of colored products from the reactions of cannabinoids with fast blue RR. *Molecules* **2025**, *30*, 3462. [[CrossRef](#)] [[PubMed](#)]
14. Hanuš, L.O.; Meyer, S.M.; Muñoz, E.; Tagliabue, S.; Scafati, O.; Appendino, G. Phytocannabinoids: A unified critical inventory. *Nat. Prod. Rep.* **2016**, *33*, 1357–1392. [[CrossRef](#)] [[PubMed](#)]
15. Tanaka, R.; Kikura-Hanajiri, R. Identification of hexahydrocannabinol (HHC), dihydro-*iso*-tetrahydrocannabinol (dihydro-*iso*-THC) and hexahydrocannabiphorol (HHCP) in electronic cigarette cartridge products. *Forensic Toxicol.* **2024**, *42*, 71–81. [[CrossRef](#)] [[PubMed](#)]
16. Webster, G.R.B.; Sarna, L.P.; Mechoulam, R. Conversion of CBD to Δ^8 -THC and Δ^9 -THC. U.S. Patent 7399872B2, 15 July 2008.
17. Choi, Y.H.; Hazekamp, A.; Peltenburg-Looman, A.M.G.; Frédérick, M.; Erkelens, C.; Lefeber, A.W.M.; Verpoorte, R. NMR assignments of the major cannabinoids and cannabiflavonoids isolated from flowers of *Cannabis sativa*. *Phytochem. Anal.* **2004**, *15*, 345–354. [[CrossRef](#)] [[PubMed](#)]
18. Yeom, H.S.; Li, H.; Tang, Y.; Hsung, R.P. Total syntheses of cannabicyclol, clusiacyclol A and B, iso-eriobrucinol A and B, and eriobrucinol. *Org. Lett.* **2013**, *15*, 3130–3133. [[CrossRef](#)] [[PubMed](#)]
19. Lavi, Y.; Kogan, N.M.; Topping, L.M.; Liu, C.; McCann, F.E.; Williams, R.O.; Breuer, A.; Yekhtin, Z.; Ezra, A.F.; Gallily, R.; et al. Novel synthesis of C-methylated phytocannabinoids bearing anti-inflammatory properties. *J. Med. Chem.* **2023**, *66*, 5536–5549. [[CrossRef](#)] [[PubMed](#)]

Disclaimer/Publisher’s Note: The statements, opinions and data contained in all publications are solely those of the individual author(s) and contributor(s) and not of MDPI and/or the editor(s). MDPI and/or the editor(s) disclaim responsibility for any injury to people or property resulting from any ideas, methods, instructions or products referred to in the content.